IDSA · Infectious Diseases Society of America   hivma · hiv medicine association   OXFORD

Early Initiation of Antiretroviral Therapy Preserves the Metabolic Function of CD4+ T Cells in Subtype C Human Immunodeficiency Virus 1 Infection

Kewreshini K. Naidoo,[1,2] Andrew J. Highton,[3] Omolara O. Baiyegunhi,[4] Sindiswa P. Bhengu,[1] Krista L. Dong,[5,6,7] Madeleine J. Bunders,[2,8] Marcus Altfeld,[2,9] and Thumbi Ndung'u[1,4,5,10,ORCID]

[1]HIV Pathogenesis Programme, The Doris Duke Medical Research Institute, University of KwaZulu-Natal, Durban, South Africa; [2]Department of Virus Immunology, Leibniz Institute of Virology, Hamburg, Germany; [3]Department of Microbiology and Immunology, University of Otago, Dunedin, New Zealand; [4]Africa Health Research Institute, Durban, South Africa; [5]Ragon Institute of Massachusetts General Hospital, Massachusetts Institute of Technology and Harvard University, Cambridge, Massachusetts, USA; [6]Division of Infectious Diseases, Massachusetts General Hospital, Boston, Massachusetts, USA; [7]Harvard Medical School, Boston, Massachusetts, USA; [8]III Department of Medicine, University Medical Center Hamburg-Eppendorf, Hamburg, Germany; [9]German Center for Infection Disease (DZIF), Partner Site Hamburg-Lübeck-Borstel-Riems, Germany; and [10]Division of Infection and Immunity, University College London, London, United Kingdom

Background. Immune dysfunction often persists in people living with human immunodeficiency virus (HIV) who are on antiretroviral therapy (ART), clinically manifesting as HIV-1-associated comorbid conditions. Early ART initiation may reduce incidence of HIV-1–associated immune dysfunction and comorbid conditions. Immunometabolism is a critical determinant of functional immunity. We investigated the effect of HIV-1 infection and timing of ART initiation on CD4+ T cell metabolism and function.

Methods. Longitudinal blood samples from people living with HIV who initiated ART during hyperacute HIV-1 infection (HHI; before peak viremia) or chronic HIV-1 infection (CHI) were assessed for the metabolic and immune functions of CD4+ T cells. Metabolite uptake and mitochondrial mass were measured using fluorescent analogues and MitoTracker Green accumulation, respectively, and were correlated with CD4+ T cell effector functions.

Results. Initiation of ART during HHI prevented dysregulation of glucose uptake by CD4+ T cells, but glucose uptake was reduced before and after ART initiation in CHI. Glucose uptake positively correlated with interleukin-2 and tumor necrosis factor-α production by CD4+ T cells. CHI was associated with elevated mitochondrial mass in effector memory CD4+ T cells that persisted after ART and correlated with PD-1 expression.

Conclusions. ART initiation in HHI largely prevented metabolic impairment of CD4+ T cells. ART initiation in CHI was associated with persistently dysregulated immunometabolism of CD4+ T cells, which was associated with impaired cellular functions and exhaustion.

Keywords. immune dysfunction; acute HIV-1 infection; CD4+ T cells; immunometabolism; antiretroviral therapy.

Human immunodeficiency virus (HIV)–associated immune activation results in progressive depletion and functional impairment of CD4+ T cells [1–3]. Antiretroviral therapy (ART) promotes quantitative and functional CD4+ T cell recovery in people living with HIV (PLWH), but reconstitution is often better in individuals who initiate ART early [4–6], although the specific mechanisms are not well defined. Cellular immune metabolism is integral to antiviral responses and there is

evidence to suggest dysregulation of these functions during HIV-1 infection [7, 8]. Harnessing immunometabolism may therefore offer potential therapeutic strategies for ART-suppressed PLWH and necessitates better understanding of the relationship between cellular metabolism and immunity in the context of HIV-1 infection.

Quiescent naive and memory T cells rely on mitochondrial oxidative phosphorylation for cell maintenance and undergo substantial metabolic reprogramming to meet the energetic and biosynthetic demands of transitioning into effector T cells [7]. Findings of a few studies investigating cellular immune metabolism in PLWH suggest that CD4+ T cells gain a highly glycolytic profile characterized by increased expression of glucose transporter, hexokinase activity, and lactate production [9, 10], and exhibit impaired mitochondrial respiration that is associated with CD4+ T cell apoptosis and depletion [11–13]. Metabolic impairments of CD4+ T cells are only partially corrected by ART [10, 12, 13], and the impact of the timing of ART initiation on CD4+ T cell metabolism remains unknown. We investigated

https://doi.org/10.1093/infdis/jiad432

the consequences of ART initiation during hyperacute HIV-1 infection (HHI) or chronic HIV-1 infection (CHI) on the metabolic and immune function of CD4$^+$ T cells in PLWH.

METHODS AND MATERIALS

Study Participants

Participants were from the Females Rising through Education, Support and Health (FRESH) [14, 15] or HIV Pathogenesis Programme Acute Infection cohorts [16]. Studies were approved by the Biomedical Research Ethics Committee of the University of KwaZulu-Natal. Participants gave written informed consent. Participants were grouped as HHI, initiating ART upon HIV-1 RNA detection (Fiebig stage I–II [HIV-1 RNA positive, p24 antigen negative/positive, and HIV-1 antibody negative]), or initiating ART during CHI (complete Western blot profile). Similar ART regimens were administered to treated HHI and CHI groups, with the exception of raltegravir, which was administered to individuals treated during HHI until 90 days after viral suppression (Supplementary Table 1). Cryopreserved peripheral blood mononuclear cell (PBMC) samples were obtained before and after ART. Controls were pre-infection PBMCs from the HHI group.

Cellular Metabolite Analogue Uptake and Mitochondrial Mass Characterization

Metabolic assays were performed as described elsewhere [17–19]. PBMCs were cultured in glucose-free Roswell Park Memorial Institute 1640 medium supplemented with 50 µM 2-deoxy-2-(7-nitro-21,3-benzoxadiazol-4-yl)amino-D-glucose (2-NBDG [glucose]) or phosphate-buffered saline supplemented with 0.125 µM 4,4-difluoro-5,7-dimethyl-4-bora-3a,4a-diaza-s-indacene-3-hexadecanoic acid (BODIPY FL C$_{16}$ [fatty acids]) for 30 minutes, or Hanks' Balanced Salt Solution supplemented with 200 µM L-kynurenine (large neutral amino acids via SLC7A5) for 4 minutes at 37°C and 5% carbon dioxide (CO$_2$). To assess mitochondrial mass (MM), PBMCs were incubated in R10-medium supplemented with 100 nM MitoTracker Green (MTG) for 30 minutes at 37°C and 5% CO$_2$. Next, PBMCs were stained for viability and with CD3, CD4, CD8, CD14, CD19, CD45RA, and CCR7 antibodies, fixed with 1% paraformaldehyde, and acquired using a BD LSRFortessa cell analyzer. 2-NBDG, BODIPY FL C$_{16}$ and MTG were detected in the fluorescein isothiocyanate (FITC) channel. L-kynurenine was detected in the Brilliant Violet (BV) 421 channel (Supplementary Table 2).

Agilent Seahorse Cell Mito Stress Test

The Agilent Seahorse Cell Mito Stress Test (Agilent Technologies) was performed to measure the bioenergetic profiles of PBMC samples. Briefly, PBMCs were cultured in either R10-medium alone or supplemented with 1 µg each of purified anti-CD3 and anti-CD28 antibodies for 18 hours at 37°C and 5% CO$_2$. Subsequently, PBMCs were resuspended in Cell Mito Stress Test medium, transferred to a Cell-Tak–coated Seahorse XFe96 cell culture microplate and incubated under CO$_2$-free conditions at 37°C for 30 minutes. Extracellular flux was measured in a Seahorse Xfe96 analyzer in the presence of mitochondrial modulators, as described elsewhere [20]. Samples were measured in triplicate. Readings were normalized to the cell counts using the BioTek Cytation cell imager (Agilent) (Supplementary Table 2).

Functional Intracellular Staining

PBMCs were cultured in R10-medium supplemented with 1 µg each of purified anti-CD3 and anti-CD28 antibodies and brefeldin A for 18 hours at 37°C and 5% CO$_2$. PBMCs were subsequently stained for viability and with CD3, CD4, CD8, CD14, CD19, CD45RA, CCR7, HLA-DR, CD38, and PD-1 antibodies, fixed with FIX & PERM medium A, permeabilized with FIX & PERM medium B, and stained with interleukin-2 (IL-2) and tumor necrosis factor (TNF)-α antibodies, before acquisition using a BD LSRFortessa cell analyzer (Supplementary Table 2).

Software and Statistical Analysis

FlowJo software, version 9.8.5, was used for flow cytometry data analysis. Seahorse Wave Desktop Software, version 2.6.0.31, was used for Seahorse Cell Mito Stress Test data analysis. GraphPad Prism software, version 9.0.1, was used for statistical analyses and graphical display. Kruskal-Wallis test with the Dunn's test for multiple comparisons was used for comparing >2 groups. Wilcoxon matched-pairs signed rank test and Mann-Whitney test were used for comparing 2 groups with paired and unpaired values, respectively. Associations were examined using Spearman rank correlation. Differences were considered statistically significant at $P < .05$.

RESULTS

Viral Suppression and CD4$^+$ T Cell Recovery in Study Participants

To investigate the impact of ART timing on the metabolic function of T cells, participants initiating ART during HHI or CHI were assessed. Of these participants, 33 (91%) were female (100% in HHI and 83% in CHI groups). The median age at ART commencement (interquartile range [IQR]) was 21 (20–22) and 23 (20–24) years in the HHI and CHI groups, respectively (Table 1). In the HHI group, the median viral load (IQR) was 4.28 (3.89–5.31) log$_{10}$ copies/mL at ART initiation, and this was suppressed below the detection limit within 2 months on ART (Supplementary Figure 1A, left). The median viral load (IQR) in the CHI group was 3.91 (3.61–4.24) log$_{10}$ copies/mL before ART, with most participants suppressed within 3–4 months on ART (Supplementary Figure 1A, right).

The median CD4$^+$ T cell count (IQR) was 927 cells/µL (799–1020 cells/µL) in the HHI group before infection, declining to

Table 1. Participant Characteristics

Characteristic	HIV Uninfected	HHI				CHI		
		ART Naive	After 2 mo of ART	After 6 mo of ART	After 12 mo of ART	ART Naive	After 6 mo of ART	After 12 mo of ART
Sex		Female, n = 18				Female, n = 15; male, n = 3		
Age at ART initiation, years		21 (20–22)				23 (20–24)		
Viral load, log$_{10}$ RNA copies/mL	NA	4.28 (3.89–5.31)	<20	<20	<20	3.91 (3.61–4.24)	<20	<20
CD4$^+$ T cell count, cells/µL	927 (799–1020)	636 (448–800)	736 (656–986)	811 (618–917)	828 (732–1000)	599 (473–719)	677 (580–793)	752 (669–926)
CD8$^+$ T cell count, cells/µL	551 (428–836)	431 (333–845)	477 (400–849)	470 (334–733)	585 (382–939)	841 (660–1135)	671 (512–778)	658 (530–769)

Data represent median (IQR) values.

Abbreviations: ART, antiretroviral therapy; CHI, chronic HIV-1 infection; HHI, hyperacute HIV-1 infection; HIV, human immunodeficiency virus; IQR, interquartile range; NA, not applicable.

636 cells/µL (448–800 cells/µL) within the first week of HIV-1 RNA detection (Supplementary Figure 1B, left), and 599 cells/µL (473–719 cells/µL) in the CHI group before ART (Supplementary Figure 1B, right), both significantly lower than in uninfected individuals (Supplementary Figure 1C). CD4$^+$ T cell counts were comparable in uninfected and HIV-infected groups 12 months after ART; however, the dynamics of recovery differed. ART during HHI allowed for rapid recovery of CD4+ T cells within 2 months (Supplementary Figure 1D, left), whereas individuals with CHI showed gradual CD4$^+$ T cell recovery after treatment, with recovery more rapid 6 months after ART initiation (Supplementary Figure 1D, right). Together, these data demonstrate rapid viral suppression when ART was initiated during HHI coupled with rapid CD4$^+$ T cell recovery, while ART initiation during CHI required a longer time to fully suppress viremia and was associated with slower CD4$^+$ T cell recovery.

Compromised Metabolite Analogue Uptake by CD4$^+$ T Cells in HIV-1 Infection with Partial Correction Following ART Initiation

Metabolic processes are integral to the optimal functioning of immune cells [7]. There is, however, a paucity of data on the consequences of HIV and the timing of ART initiation for immune cell metabolism. We therefore investigated T cell capacities to internalize essential nutrients in participant groups by flow cytometry (Supplementary Figure 2). Glucose, fatty acid, and amino acid uptake were measured using fluorescent metabolite analogues 2-NBDG, BODIPY FL C$_{16}$, and L-kynurenine, respectively (Figure 1A–1C, left). In uninfected individuals, delineation by CD4$^+$ T cell subsets showed that metabolite analogue uptake was relatively low in naive CD4$^+$ T cells and that uptake was predominantly by memory subsets, particularly CD4$^+$ effector memory T (T$_{EM}$) and terminal effector memory T (T$_{TEM}$) cells (Figure 1A–1C, middle).

Assessment was extended to HHI and CHI groups to determine the impact of HIV-1 infection and ART timing on metabolite analogue uptake by total CD4$^+$ T cells (Figure 1A–1C, right). 2-NBDG uptake was comparable in individuals with HHI before and during early infection preceding ART and remained stable after ART (Figure 1A, right). In contrast, individuals with CHI displayed lower 2-NBDG uptake at baseline than uninfected individuals and those with HHI before ART, and this difference compared to the HHI group persisted up to 12 months on ART (Figure 1A, right). BODIPY FL C$_{16}$ uptake by CD4$^+$ T cells was significantly lower in both untreated HIV-1–infected groups than in uninfected individuals (Figure 1B, right), but improved after ART initiation so that BODIPY FL C$_{16}$ uptake in HHI and CHI groups was similar to that in the HIV-1–negative group ($P > .05$ for all comparisons). L-kynurenine uptake by CD4$^+$ T cells was largely unaffected by HIV-1 infection (Figure 1C, right). It should be noted, however, that although L-kynurenine uptake was not significantly affected by HIV infection, this does not exclude the possibility that uptake of other amino acids, such as glutamine, are affected owing to their uptake by other transporters [21].

No associations were observed between total CD4$^+$ T cell metabolite analogue uptake and viral load or CD4$^+$ T cell count before ART initiation in HIV-infected groups (Supplementary Figure 3). Further analysis showed no significant differences in metabolite analogue uptake by total CD8$^+$ T cells between PLWH before and after ART compared to uninfected individuals (Supplementary Figure 4A–4C). Lower 2-NBDG uptake in untreated CHI was observed in CD8$^+$ T$_{EM}$ cells ($P = .004$; data not shown); however, this function was reconstituted after ART initiation and was then comparable to 2-NBDG uptake by CD8$^+$ T$_{EM}$ cells in uninfected individuals ($P = .13$; data not shown). Collectively, the data showed only minor changes in CD8$^+$ T cells but suggest that glucose and fatty acid uptake by CD4$^+$ T cells is impaired during untreated HIV-1 infection, independent of viremia or CD4$^+$ T cell count.
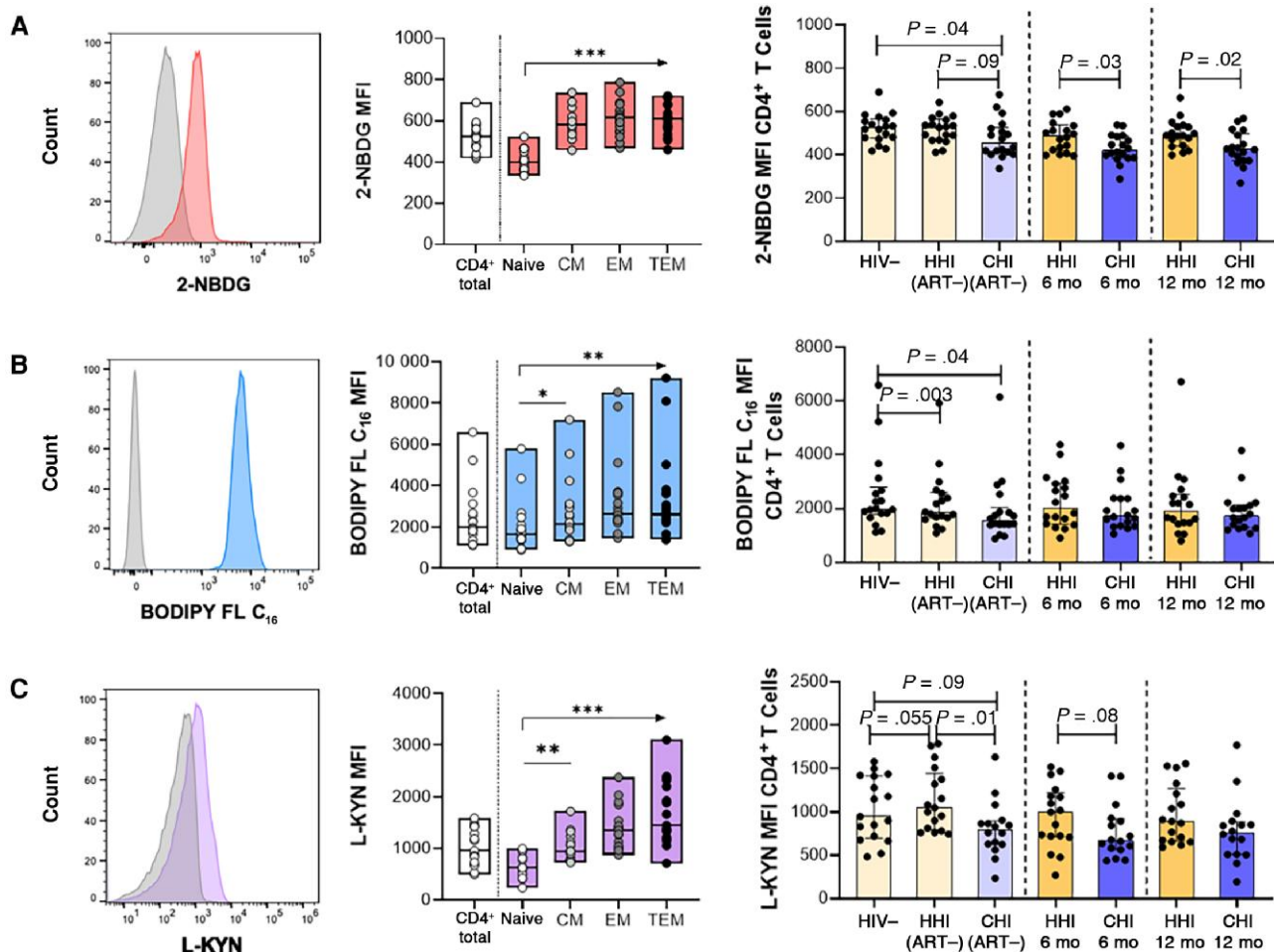
Figure 1. Compromised metabolite analogue uptake by CD4+ T cells in human immunodeficiency virus (HIV)-1 infection with partial correction following antiretroviral therapy (ART) initiation. *A, Left,* Representative histogram of 2-deoxy-2-(7-nitro-21,3-benzoxadiazol-4-yl)amino-D-glucose (2-NBDG) uptake (glucose) compared with Fluorescence Minus One (FMO) control in CD4+ T cells. *Middle,* 2-NBDG uptake in CD4+ T cells and subsets in the HIV-1–negative (HIV−) group. *Right,* Comparison of 2-NB-DG uptake in CD4+ T cells between hyperacute HIV-1 infection (HHI) and chronic HIV-1 infection (CHI) groups before and after ART. *B, Left,* Representative histogram of 4,4-difluoro-5,7-dimethyl-4-bora-3a,4a-diaza-s-indacene-3-hexadecanoic acid (BODIPY FL C_{16}) uptake (lipids) compared with FMO control in CD4+ T cells. *Middle,* BODIPY FL C_{16} uptake in CD4+ T cells and subsets in the HIV− group. *Right,* Comparison of BODIPY FL C_{16} uptake in CD4+ T cells between HHI and CHI groups before and after ART. *C, Left,* Representative histogram of L-kynurenine (L-KYN) uptake (amino acids) compared with FMO control in CD4+ T cells. *Middle,* L-KYN uptake in CD4+ T cells and subsets in the HIV− group. *Right,* Comparison of L-KYN uptake in CD4+ T cells between HHI and CHI groups before and after ART. Abbreviations: 6 mo, 6 months after ART initiation; 12 mo, 12 months after ART initiation; ART−, ART naive; CM, central memory; EM, effector memory; MFI, Median Fluorescence Intensity; TEM, terminal EM. *$P < .05$; **$P < .01$; ***$P < .001$.

Initiating ART during HHI preserved the uptake of both nutrients by CD4+ T cells. Starting ART during CHI improved fatty acid uptake to levels seen in uninfected individuals but did not fully rescue glucose uptake by CD4+ T cells, which remained significantly reduced even after 12 months of ART.

Higher MM in CD4+ T_{EM} Cell Subsets in Individuals Starting ART During CHI

Most energy production occurs via oxidative phosphorylation within mitochondria. Optimal mitochondrial functioning is therefore key to effective energy production required for the regulation of T cell immune functions [22]. Mitochondrial

dynamics within T cells during HIV-1 infection in relation to ART timing was determined using fluorescent MTG as a measure of relative MM and the quantity of active mitochondria (Figure 2A, left). In uninfected individuals, MM was higher in memory CD4+ T cells than in naive cells (Figure 2A, middle). In total CD4+ T cells, no significant differences in MM were detected during HIV-1 infection, before or after ART, compared to uninfected individuals (Figure 2A, right). CD4+ T cell subset analysis showed that HIV-1 infection and ART initiation did not significantly affect MM in naive and CD4+ central memory T (T_{CM}) cells (Figure 2B, top). There was, however, substantially higher MM in both T_{EM} and T_{TEM} CD4+ T cell subsets
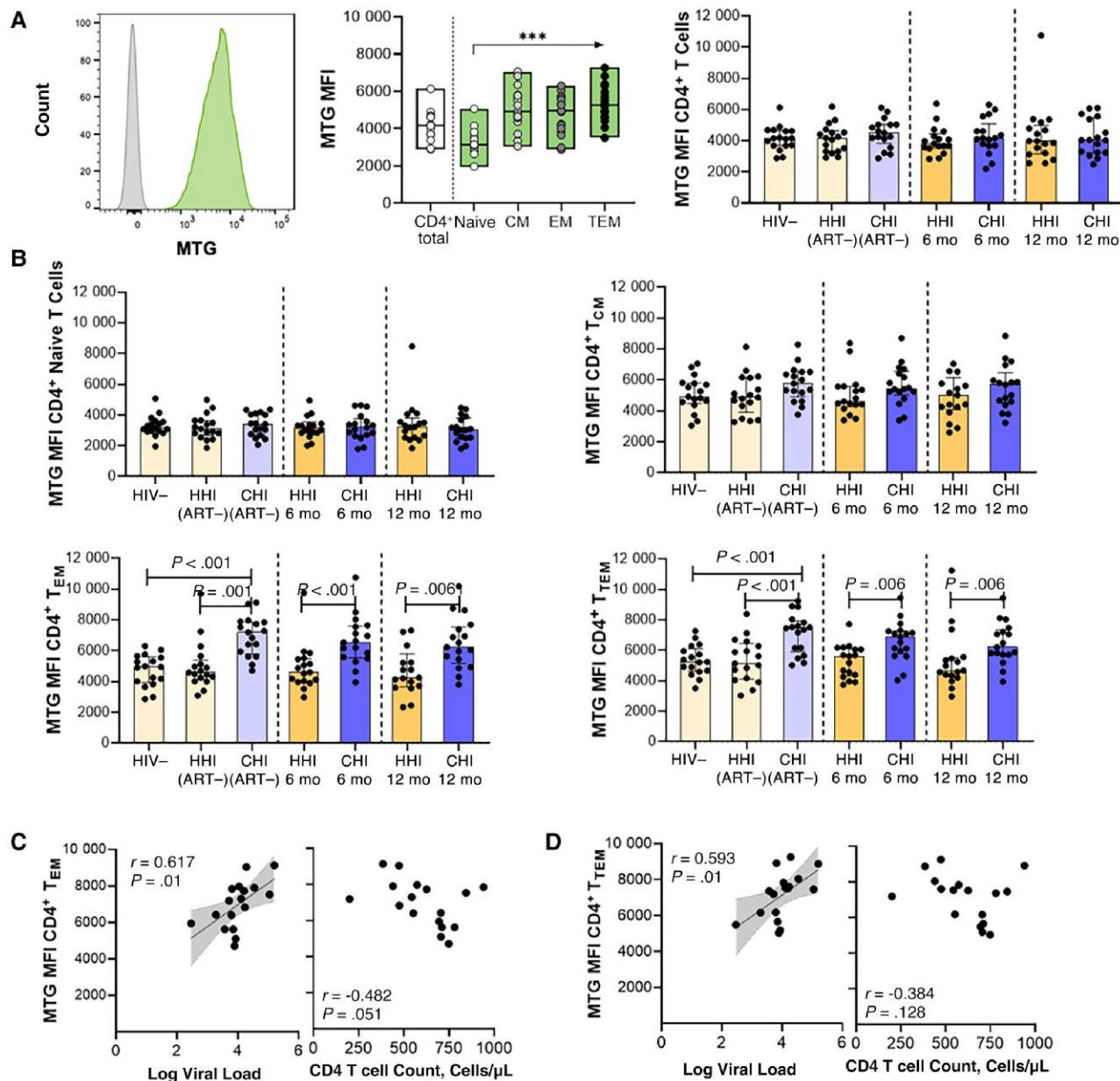
Figure 2. Higher mitochondrial mass in CD4+ effector memory T (EM) cell subsets in individuals starting antiretroviral therapy (ART) during chronic human immunodeficiency virus (HIV)-1 infection (CHI). *A, Left,* Representative histogram of MitoTracker Green FM dye (MTG) uptake compared with Fluorescence Minus One (FMO) control in CD4+ T cells. *Middle,* MTG uptake in CD4+ T cells and subsets in the HIV-1–negative (HIV−) group. *Right,* Comparison of MTG uptake in CD4+ T cells between groups with hyperacute HIV-1 infection (HHI) and CHI before and after ART. *B,* Comparison of MTG uptake in CD4+ T cell subsets, including naive (*top left*), central memory (CM; *top right*), EM (*bottom left*), and terminal EM (TEM; *bottom right*) CD4+ T cells, between HHI and CHI groups before and after ART. *C, D,* Correlations between MTG uptake in EM (*C*) and TEM (*D*) subsets in the CHI treated group before ART and viral load or CD4+ T cell count. ***P < .001. Abbreviations: 6 mo, 6 months after ART initiation; 12 mo, 12 months after ART initiation; ART−, ART naive; MFI, Median Fluorescence Intensity.

in untreated individuals with CHI than in uninfected persons and those with HHI before ART (Figure 2B, bottom). Augmented MM of CD4+ T$_{EM}$ and T$_{TEM}$ T cells in treatment-naive individuals with CHI was strongly associated with viremia (Figure 2C, left, and 2D, left) and inversely correlated with CD4+ T cell counts (Figure 2C, right).

Although MM dropped after ART, it was still significantly higher in CHI treated individuals compared to HHI treated individuals after 12 months of ART (Figure 2B, bottom). Spearman analysis revealed that 2-NBDG uptake (glucose) positively correlated with MM in total CD4+ T cells in CHI treated individuals ($r = 0.500$; $P = .04$), but this association was not observed at the CD4+ T cell subset level (naive, $r = 0.298$ and P

= .24; T_{CM}, $r = 0.339$ and $P = .18$; T_{EM}, $r = 0.288$ and $P = .26$; T_{TEM}, $r = 0.259$ and $P = .31$; data not shown). Next, MTG signal was measured in $CD8^+$ T cells; here, significantly higher MM was observed in untreated individuals with CHI, in total $CD8^+$ T cells (Supplementary Figure 4D) and $CD8^+$ T cell subsets (naive, $P = .08$; T_{CM}, $P = .01$; T_{EM}, $P = .02$; $T_{terminally differentiated effector memory cells re-expressing CD45RA (TEMRA)}$, $P = .03$; data not shown). Relative MM decreased after ART initiation in the $CD8^+$ T cells of CHI treated individuals, and after 12 months of ART was comparable to that of uninfected individuals.

To further investigate mitochondrial changes induced by HIV infection, we performed the Cell Mito Stress Test to measure the oxygen consumption rate profiles in PBMCs from uninfected individuals and CHI treated individuals, either without or after T cell receptor (TCR) stimulation (Supplementary Figure 5A). Basal respiration tended to be higher in those with CHI before ART initiation for unstimulated and stimulated conditions ($P = .055$; data not shown), but no differences in maximal respiration were observed between uninfected and HIV-infected individuals (no stimulation, $P = .17$; TCR stimulated, $P = .40$; data not shown). Importantly, the percentage spare respiratory capacity, which reflects the reserve mitochondrial respiration capacity that is available to the cell under stress-induced conditions, was lower in individuals with CHI before and during ART, compared to the HIV-negative group (Supplementary Figure 5B), suggestive of persistent mitochondrial dysregulation in individuals that initiated ART during CHI. Together, the data show reduced mitochondrial spare respiratory capacity of PBMCs and elevated MM in $CD4^+$ T_{EM} and T_{TEM} cells associated with viremia in CHI that persisted after ART-induced viral suppression, indicating dysregulated mitochondrial activity in CHI treated individuals, even after 12 months on ART.

Association Between Metabolic Dysregulations and Repressed Immune Functions of $CD4^+$ T Cells in Individuals Initiating ART During CHI

After observing metabolic dysregulations of $CD4^+$ T cells in CHI that persisted up to 12 months after ART initiation, we assessed the impact of altered glucose uptake and MM on $CD4^+$ T cell immune functions. $CD4^+$ T cells were assessed for coinhibitory receptor PD-1 expression that is essential for lymphocyte homeostasis signaling and is associated with T cell exhaustion in HIV-1 infection [23, 24]. PD-1 expression was highest in memory $CD4^+$ T cells, particularly $CD4^+$ T_{EM} cells, in uninfected individuals (Figure 3A, left) and CHI individuals after 12 months of ART (Figure 3A, right). Furthermore, PD-1 expression in $CD4^+$ T_{EM} cells was significantly higher in CHI compared to uninfected controls ($P = .007$; data not shown).

We therefore focused subsequent analysis on potential associations between PD-1 expression and metabolic dynamics of $CD4^+$ T_{EM} cells in uninfected individuals and CHI treated individuals in whom we had observed persistent metabolic dysregulations. The percentage of $PD-1^+$ $CD4^+$ T_{EM} cells strongly correlated with MM ($r = 0.612$; $P < .001$) yet only weakly associated with 2-NBDG uptake ($r = 0.211$; $P = .12$; data not shown) of $CD4^+$ T_{EM} cells. Further assessment of MM and PD-1-expression in $CD4^+$ T_{EM} cells in the different groups revealed a positive correlation in uninfected individuals but also in individuals with CHI before and after treatment, in which both MM and the percentage of $PD-1^+$ $CD4^+$ T_{EM} cells were higher (Figure 3B). These data demonstrate that elevated MM in $CD4^+$ T_{EM} cells observed in CHI was associated with up-regulation of the exhaustion marker PD-1.

We next assessed the functional ability of $CD4^+$ T cells to respond to TCR stimulation and correlated these effector functions with glucose uptake and MM. PBMCs cultured with purified anti-CD3 and anti-CD28 antibodies were measured for IL-2 and TNF-α production by $CD4^+$ T cells using flow cytometry (Figure 3C, left, and 3D, left). Lower percentages of $CD4^+$ T cells produced IL-2 (Figure 3C, middle]) and TNF-α (Figure 3D, middle) in individuals with CHI compared to uninfected individuals, even after 12 months of ART. Furthermore, the percentages of both IL-2– and TNF-α–producing $CD4^+$ T cells positively correlated with 2-NBDG uptake by $CD4^+$ T cells in the HIV-1–negative group and the CHI group 12 months after ART initiation (Figure 3C, right, and 3D, right), in line with the need to generate energy through glycolysis for cytokine production. Collectively, the data show that glucose uptake and associated cytokine production were impaired in individuals starting ART during CHI, even after 12 months of ART. In contrast, MM of $CD4^+$ T cells were not correlated with the percentage of cytokine-producing $CD4^+$ T cells (Supplementary Figure 6), indicating distinct but synergistic consequences of persistent impairments of glucose uptake and MM in $CD4^+$ T cells on function and expression of checkpoint inhibitors.

DISCUSSION

We explored the consequences of HIV-1 infection and ART timing on the metabolic function of T cells in PLWH from South Africa. The timing of ART initiation was associated with distinct viral load and $CD4^+$ T cell recovery dynamics, with rapid virus suppression and faster $CD4^+$ T cell rebound when ART was started in HHI. However, after 12 months of ART, $CD4^+$ T cell counts in both HIV-treated groups were comparable to those of uninfected individuals, suggestive of quantitative $CD4^+$ T cell reconstitution irrespective of ART timing. Despite this, we provide evidence that metabolic functioning of $CD4^+$ T cells during HIV-1 infection is highly dependent on the timing of ART. Using metabolite surrogates, we demonstrate that ART initiation during HHI preserved nutrient uptake and MM of $CD4^+$ T cells. In contrast, untreated CHI was associated with compromised nutrient uptake by
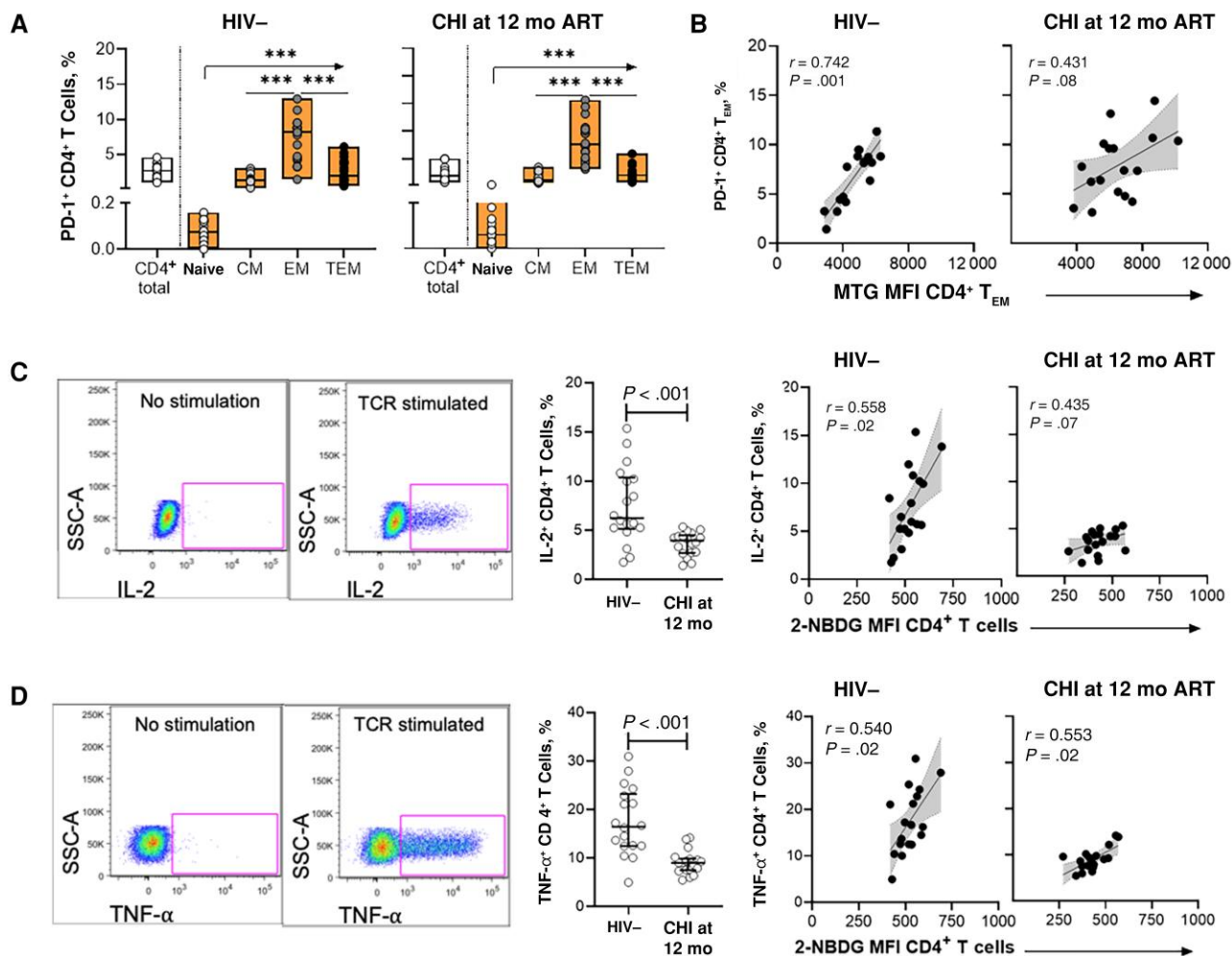
Figure 3. Metabolic dysregulations are associated with reduced cytokine production and cellular exhaustion of CD4+ T cells in individuals initiating antiretroviral therapy (ART) during chronic human immunodeficiency virus (HIV)-1 infection (CHI). *A,* Frequency of PD-1+ CD4+ T cells and subsets in the HIV-1–negative (HIV–) group (*left*) and CHI treated group at 12 months after ART initiation (*right*). *B,* Correlations between frequency of PD-1+ CD4+ effector memory T (T_{EM}) cells and MitoTracker Green FM dye (MTG) uptake in CD4+ T_{EM} cells. *C, Left,* Representative gating strategy showing interleukin-2 (IL-2) production by CD4+ T cells without or with stimulation. *Middle,* Comparison of IL-2 production by T cell receptor (TCR)–stimulated CD4+ T cells between the HIV– group and the CHI treated group at 12 months after ART initiation. *Right,* Correlations between IL-2 production and glucose uptake by CD4+ T cells in the HIV– group and the CHI treated group at 12 months after ART initiation. *D, Left,* Representative gating strategy showing tumor necrosis factor (TNF)-α production by CD4+ T cells without or with stimulation. *Middle,* Comparison of TNF-α production by TCR-stimulated CD4+ T cells between the HIV– group and the CHI treated group after 12 months of ART. *Right,* Correlations between TNF-α production and glucose uptake by CD4+ T cells in the HIV– group and the CHI treated group after 12 months of ART. ***$P < .001$. Abbreviations: 12 mo, 12 mo after ART initiation; CM, central memory; MFI, Median fluorescence intensity; SSC, side scatter; TEM, terminal EM.

CD4+ T cells and higher MM in CD4+ T_{EM} cells. Starting ART during CHI improved lipid uptake by CD4+ T cells to levels observed in uninfected individuals, but reduced glucose uptake and elevated MM in CD4+ T cells persisted following ART. Assessment of these metabolic dysregulations in relation to immune function revealed that impaired 2-NBDG uptake was associated with lower capacity of CD4+ T cells to produce effector cytokines, while higher MM correlated with up-regulated PD-1 expression in CD4+ T_{EM} cells in CHI treated individuals. These results demonstrate that the timing of ART initiation can affect the metabolic reconstitution of CD4+ T cells.

Metabolism of essential nutrients is central to immune cellular functioning and dependent on nutrient availability [25, 26]. We report impediment of 2-NBDG and BODIPY FL C_{16} uptake by CD4+ T cells, suggestive of impaired glucose and fatty acid uptake, in untreated CHI. Limited studies exploring the metabolic capacities of CD4+ T cells from PLWH have focused on markers of glucose metabolism [9, 12]. Intensified glycolysis in CD4+ T cells has been demonstrated by an up-regulation of glucose transporter and higher 2-NBDG internalization during treatment-naive CHI, and was not fully remedied by ART [9, 10]. Comparing the metabolic findings reported here with

past studies necessitates caution. Sex and age disparities of cohorts that can affect metabolism regulation, immunity, and antiviral responses need to be considered, with predominantly young female participants with relatively high CD4$^+$ T cell counts included in the current study, compared to previous studies that included mainly older all-male cohorts, often with lower CD4$^+$ T cell counts [27–29]. Furthermore, the metabolic dysregulations resulting from different ART regimens in PLWH need to be considered (reviewed in [30]). Similar ART regimens were administered to HHI and CHI treated groups, with the exception of raltegravir, which was administered to HHI treated individuals until 90 days after viral suppression; however, raltegravir has not previously been associated with severe metabolic perturbations after short-term therapy [31], and we did not observe any persistent metabolic dysregulations in individuals that started treatment during HHI. Other differences, including ethnicity and diet, may also influence differential metabolic programming during infection [32], and the lack of clinical information regarding body mass index, blood glucose levels, and diabetes diagnoses in study participants represents a limitation of the current study. Importantly, our study design enabled us to assess the impact of ART timing on nutrient uptake of CD4$^+$ T cells. ART initiation during HHI prevented impairments of nutrient uptake in CD4$^+$ T cells, while starting ART during CHI only enabled reconstitution of fatty acid internalization while impaired glucose uptake by CD4$^+$ T cells persisted.

Glucose is a critical nutrient for all stages of cellular respiration. Reduced glucose uptake by CD4$^+$ T cells when ART was started during CHI may therefore affect mitochondria, the powerhouses of cellular respiration. MM was highest within CD4$^+$ T cell memory subsets versus naive cells irrespective of HIV status. No differences were observed in the MM of total CD4$^+$ T cells between CHI treated PLWH and uninfected counterparts, consistent with previous findings [10]; however, significantly higher accumulation of mitochondria in the CD4$^+$ T$_{EM}$ cells of treatment-naive persons with CHI was observed and was positively correlated with viremia, suggestive of disrupted homeostatic mitochondrial biogenesis in response to chronic antigenic stimulation. There was only incremental waning of MM following ART, such that elevated MM in these cellular subsets of CHI treated people was still observed 12 months after ART initiation, suggesting that once viral replication is suppressed, the mitochondrial activity of CD4$^+$ T$_{EM}$ cells in CHI treated individuals takes longer to stabilize. Mitochondrial respiration levels in CD4$^+$ T cells were previously found to be lower before and after ART-controlled infection [12, 13], providing insight into the detrimental effects of HIV-1 on mitochondrial dynamics in CD4$^+$ T cells that are not resolved with ART. Our data show that early ART initiation has an advantageous impact in preserving the mitochondrial dynamics of CD4$^+$ T cells,

an observation that might explain the described clinical benefit of early ART initiation [33].

Indications of compromised glucose uptake and MM modulation in CD4$^+$ T cells of chronically treated PLWH led us to investigate the effect of these metabolic irregularities on CD4$^+$ T cell functionality. TCR-induced cytokine production, specifically for IL-2 and TNF-α, was significantly inferior in CHI treated individuals, even after 12 months on ART. Impaired cytokine production significantly associated with reduced CD4$^+$ T cell glucose uptake, in line with glucose being a key metabolite for effector molecule production [34]. Furthermore, PD-1 expression was up-regulated on CD4$^+$ T$_{EM}$ cells in all groups, and higher MM was associated with higher frequencies of PD-1–expressing CD4$^+$ T$_{EM}$ cells in CHI treated individuals before and after ART. Antigen persistence induces the up-regulation of immune checkpoint inhibitors, including PD-1, in T cells in an effort to attenuate persistent signaling downstream of the TCR. In chronic lymphocytic choriomeningitis virus mouse models, PD-1 signaling during early T cell exhaustion exerted glycolytic and mitochondrial alterations that ultimately dysregulated mitochondrial biogenesis [35]. Thus, dysregulated MM in CD4$^+$ T$_{EM}$ cells in PLWH due to chronic immune activation and higher PD-1 signaling may represent an early precursor marker to cellular exhaustion.

Collectively our data reveal metabolic mechanisms that account for variable functional recovery of CD4$^+$ T cells in a population group with high HIV-1 infection burden in sub-Saharan Africa; and highlight the beneficial effects of early ART administration in averting metabolic alterations to CD4$^+$ T cells, at least within the first year of ART. The study emphasizes the complexity of immunometabolism that warrants further investigation and may require population-specific approaches for complementary therapeutic interventions in ART-suppressed PLWH.

Supplementary Data

Supplementary materials are available at *The Journal of Infectious Diseases* online. Consisting of data provided by the authors to benefit the reader, the posted materials are not copyedited and are the sole responsibility of the authors, so questions or comments should be addressed to the corresponding author.

Notes

Author contributions. Concept and study design: K. L. D., M. J. B., M. A., and T. N. Data collection, experimental optimization and acquisition: K. K. N., A. J. H., O. O. B., S. P. B., and K. L. D. Analysis and interpretation of data: K. K. N., M. A., and T. N. Drafting of the manuscript: K. K. N., M. A., and T. N.

References

1. Paiardini M, Müller-Trutwin M. HIV-associated chronic immune activation. Immunol Rev **2013**; 254:78–101.
2. Okoye AA, Picker LJ. CD4$^+$ T-cell depletion in HIV infection: mechanisms of immunological failure. Immunol Rev **2013**; 254:54–64.
3. Mazzuti L, Turriziani O, Mezzaroma I. The many faces of immune activation in HIV-1 infection: a multifactorial interconnection. Biomedicines **2023**; 11:159.
4. Le T, Wright EJ, Smith DM, et al. Enhanced CD4+ T-cell recovery with earlier HIV-1 antiretroviral therapy. N Engl J Med **2013**; 368:218–30.
5. Wilson EM, Sereti I. Immune restoration after antiretroviral therapy: the pitfalls of hasty or incomplete repairs. Immunol Rev **2013**; 254:343–54.
6. Sun Y, Fu Y, Zhang Z, et al. The investigation of CD4$^+$ T-cell functions in primary HIV infection with antiretroviral therapy. Medicine (Baltimore) **2017**; 96:e7430.
7. Shehata HM, Murphy AJ, Lee MS, et al. Sugar or fat? metabolic requirements for immunity to viral infections. Front Immunol **2017**; 8:1311.
8. Sáez-Cirión A, Sereti I. Immunometabolism and HIV-1 pathogenesis: food for thought. Nat Rev Immunol **2021**; 21:5–19.
9. Palmer CS, Ostrowski M, Gouillou M, et al. Increased glucose metabolic activity is associated with CD4$^+$ T-cell activation and depletion during chronic HIV infection. AIDS **2014**; 28:297–309.
10. Masson JJR, Murphy AJ, Lee MKS, Ostrowski M, Crowe SM, Palmer CS. Assessment of metabolic and mitochondrial dynamics in CD4+ and CD8+ T cells in virologically suppressed HIV-positive individuals on combination antiretroviral therapy. PLoS One **2017**; 12:e0183931.
11. Arnoult D, Petit F, Lelièvre JD, Estaquier J. Mitochondria in HIV-1-induced apoptosis. Biochem Biophys Res Commun **2003**; 304:561–74.
12. Korencak M, Byrne M, Richter E, et al. Effect of HIV infection and antiretroviral therapy on immune cellular functions. JCI Insight **2019**; 4:e126675.
13. Zhao J, Schank M, Wang L, et al. Mitochondrial functions are compromised in CD4 T cells from ART-controlled PLHIV. Front Immunol **2021**; 12:658420.
14. Dong KL, Moodley A, Kwon DS, et al. Detection and treatment of Fiebig stage I HIV-1 infection in young at-risk women in South Africa: a prospective cohort study. Lancet HIV **2018**; 5:e35–44.
15. Ndung'u T, Dong KL, Kwon DS, Walker BD. A FRESH approach: combining basic science and social good. Sci Immunol **2018**; 3:eaau2798.
16. Bassett IV, Chetty S, Giddy J, et al. Screening for acute HIV infection in South Africa: finding acute and chronic disease. HIV Med **2011**; 12:46–53.
17. Pfeifer C, Highton AJ, Peine S, et al. Natural killer cell education is associated with a distinct glycolytic profile. Front Immunol **2018**; 9:3020.
18. Sinclair LV, Neyens D, Ramsay G, Taylor PM, Cantrell DA. Single cell analysis of kynurenine and system L amino acid transport in T cells. Nat Commun **2018**; 9:1981.
19. Highton AJ, Diercks BP, Möckl F, et al. High metabolic function and resilience of NKG2A-educated NK cells. Front Immunol **2020**; 11:559576.
20. Cumming BM, Baig Z, Addicott KW, Chen D, Steyn AJC. Host bioenergetic parameters reveal cytotoxicity of antituberculosis drugs undetected using conventional viability assays. Antimicrob Agents Chemother **2021**; 65:e0093221.
21. Scalise M, Pochini L, Console L, Losso MA, Indiveri C. The human SLC1A5 (ASCT2) amino acid transporter: from function to structure and role in cell biology. Front Cell Dev Biol **2018**; 6:96.
22. Ledderose C, Bao Y, Lidicky M, et al. Mitochondria are gate-keepers of T cell function by producing the ATP that drives purinergic signaling. J Biol Chem **2014**; 289:25936–45.
23. Day CL, Kaufmann DE, Kiepiela P, et al. PD-1 expression on HIV-specific T cells is associated with T-cell exhaustion and disease progression. Nature **2006**; 443:350–4.
24. Tkachev V, Goodell S, Opipari AW, et al. Programmed death-1 controls T cell survival by regulating oxidative metabolism. J Immunol **2015**; 194:5789–800.
25. Yuan HX, Xiong Y, Guan KL. Nutrient sensing, metabolism, and cell growth control. Mol Cell **2013**; 49:37987.
26. Newsholme P. Cellular and metabolic mechanisms of nutrient actions in immune function. Nutr Diabetes **2021**; 11:22.
27. Rubin JB, Lagas JS, Broestl L, et al. Sex differences in cancer mechanisms. Biol Sex Differ **2020**; 11:17.
28. Jacobsen H, Klein SL. Sex differences in immunity to viral infections. Front Immunol **2021**; 12:720952.

29. Martin DE, Torrance BL, Haynes L, Bartley JM. Targeting aging: lessons learned from immunometabolism and cellular senescence. Front Immunol 2021; 12:714742.

30. Thet D, Siritientong T. Antiretroviral therapy-associated metabolic complications: review of the recent studies. HIV AIDS (Auckl) 2020; 12:507–24.

31. Lake JE, McComsey GA, Hulgan TM, et al. A randomized trial of raltegravir replacement for protease inhibitor or non-nucleoside reverse transcriptase inhibitor in HIV-infected women with lipohypertrophy. AIDS Patient Care STDS 2012; 26:532–40.

32. Palmer CS. Innate metabolic responses against viral infections. Nat Metab 2022; 4:1245–59.

33. De Clercq J, Rutsaert S, De Scheerder MA, Verhofstede C, Callens S, Vandekerckhove L. Benefits of antiretroviral therapy initiation during acute HIV infection. Acta Clin Belg 2022; 77:168–76.

34. Pearce EL. Metabolism in T cell activation and differentiation. Curr Opin Immunol 2010; 22:314–20.

35. Bengsch B, Johnson AL, Kurachi M, et al. Bioenergetic insufficiencies due to metabolic alterations regulated by the inhibitory receptor PD-1 are an early driver of CD8^{+} T cell exhaustion. Immunity 2016; 45:358–73.